Residue Phe112 of the Human-Type Corrinoid Adenosyltransferase (PduO) Enzyme of *Lactobacillus reuteri* Is Critical to the Formation of the Four-Coordinate Co(II) Corrinoid Substrate and to the Activity of the Enzyme[†,‡]

Paola E. Mera,[§] Martin St Maurice,[||,⊥] Ivan Rayment,[||] and Jorge C. Escalante-Semerena*[,§]

Departments of Bacteriology and Biochemistry, University of Wisconsin, Madison, Wisconsin 53706

Received January 5, 2009; Revised Manuscript Received February 20, 2009

ABSTRACT: ATP:Corrinoid adenosyltransferases (ACAs) catalyze the transfer of the adenosyl moiety from ATP to cob(I)alamin via a four-coordinate cob(II)alamin intermediate. At present, it is unknown how ACAs promote the formation of the four-coordinate corrinoid species needed for activity. The published high-resolution crystal structure of the ACA from *Lactobacillus reuteri* (*Lr*PduO) in complex with ATP and cob(II)alamin shows that the environment around the α face of the corrin ring consists of bulky hydrophobic residues. To understand how these residues promote the generation of the four-coordinate cob(II)alamin, variants of the human-type ACA enzyme from *L. reuteri* (*Lr*PduO) were kinetically and structurally characterized. These studies revealed that residue Phe112 is critical in the displacement of 5,6-dimethylbenzimidazole (DMB) from its coordination bond with the Co ion of the ring, resulting in the formation of the four-coordinate species. An F112A substitution resulted in a 80% drop in the catalytic efficiency of the enzyme. The explanation for this loss of activity was obtained from the crystal structure of the mutant protein, which showed cob(II)alamin bound in the active site with DMB coordinated to the cobalt ion. The crystal structure of an *Lr*PduO^{F112H} variant showed a DMB-off/His-on interaction between the corrinoid and the enzyme, whose catalytic efficiency was 4 orders of magnitude lower than that of the wild-type protein. The analysis of the kinetic parameters of *Lr*PduO^{F112H} suggests that the F112H substitution negatively impacts product release. Substitutions of other hydrophobic residues in the Cbl binding pocket did not result in significant defects in catalytic efficiency in vitro; however, none of the variant enzymes analyzed in this work supported AdoCbl biosynthesis in vivo.

The chemistry of B_{12}-dependent reactions and the biosynthesis of this complex coenzyme have been an area of intense investigation for decades. Coenzyme B_{12} [adenosylcobalamin (AdoCbl)][1] and methylcobalamin (MeCbl) are the two biologically active forms of B_{12}. AdoCbl participates in radical-based intramolecular rearrangements (*1*−*3*), deaminations (*4*), dehydrations (*5*), reductions (*6, 7*), and reductive dehalogenations (*8*), while Cbl serves as a transient methyl carrier in methylation reactions (*9*−*11*). Despite the range of chemical reactions carried out by these forms of B_{12}, MeCbl and, in some cases, AdoCbl bind to enzymes in very similar conformations. For example, the crystal structures of methylmalonyl-CoA mutase (MMCM, AdoCbl-dependent) and methionine synthase (MeCbl-dependent) revealed Cbl bound in the active site in a base-off−His-on conformation (*12, 13*). In contrast, the active sites of the bacterial and human ATP:Corrinoid adenosyltransferases do not have a histidinyl residue in the proximity of the cobalt ion, suggesting that catalysis does not occur via a DMB-off/His-on intermediate.

One fascinating aspect of the corrinoid adenosylation reaction is the reduction of the Co(II) corrinoid substrate. While the environment inside the cell is sufficiently reductive to drive the reduction of Co^{3+} to Co^{2+} (*14*), it is not low enough to drive the reduction of Co^{2+} to Co^{+} (*15, 16*). ACA enzymes bind cob(II)alamin and facilitate its reduction by generating a four-coordinate cob(II)alamin species in the active site (*17*−*20*). The four-coordinate species lacks axial ligands, the absence of which stabilizes the $3d_{z^2}$ orbital and raises the Co^{2+} to Co^{+} reduction midpoint potential to within the range of reducing agents inside the cell (*17*). By binding

[†] Work in the Escalante-Semerena laboratory was supported by NIH Grant R01-GM40313 to J.C.E.-S. Work in the Rayment laboratory was supported by NIH Grant AR35186. P.E.M. was supported in part by NIH Grant NRSA F31-GM081979.

[‡] The atomic coordinates and structure factors for the complexes of *Lr*PduO^{F112H}, *Lr*PduO^{F112A}, and *Lr*PduO$^{\Delta S183}$ in complex with ATP and cob(II)alamin have been deposited in the Protein Data Bank, Research Collaboratory for Structural Bioinformatics, Rutgers University, New Brunswick, NJ, as entries 3GAH, 3GAI, and 3GAJ, respectively.

* To whom correspondence should be addressed: 1550 Linden Dr., Madison, WI 53706. Telephone: (608) 262-7379. Fax: (608) 265-7909. E-mail: escalante@bact.wisc.edu.

[§] Department of Bacteriology.

[||] Department of Biochemistry.

[⊥] Current address: Department of Biological Sciences, Marquette University, Milwaukee, WI 53201.

[1] Abbreviations: ACA, ATP:Corrinoid adenosyltransferase; *Lr*PduO, *Lactobacillus reuteri* PduO; *Se*PduO, *Salmonella enterica* PduO; Cbl, cobalamin; cbi, cobinamide; AdoCbl, adenosylcobalamin; HOCbl, hydroxycobalamin; DMB, 5,6-dimethylbenzimidazole; MMCM, methylmalonyl-CoA mutase; Tris-HCl, tris(hydroxymethyl)aminomethane hydrochloride; FMN, flavin mononucleotide; FldA, flavodoxin; Fpr, ferredoxin (flavodoxin):NADPH reductase; Fre, FMN reductase; MES, morpholinoethanesulfonic acid; NADH, reduced nicotinamide adenine dinucleotide; PDB, Protein Data Bank.

10.1021/bi9000134 CCC: $40.75
Published on Web 02/23/2009

cob(II)alamin in the active site, ACA enzymes generate a Co^+ "super-nucleophile" and prevent its quenching by deleterious side reaction. At present, however, there is no direct evidence that ACA enzymes deficient in their ability to generate the four-coordinate cob(II)alamin are impaired in catalyzing the adenosylation reaction.

The crystal structure of the *Lactobacillus reuteri* PduO enzyme in complex with ATP and cob(II)alamin confirmed the existence of the four-coordinate cob(II)alamin intermediate (*21*). The protein environment around the vacant α-axial ligand region consists of several bulky and hydrophobic residues positioned in the proximity of the cob(II)alamin substrate (*21*). The role of these residues in the generation of the four-coordinate intermediate remains unclear. Kinetic and structural analyses reported here provide insights into the role of hydrophobic residues in the generation of the four-coordinate cob(II)alamin intermediate. We also report the structure and kinetic behavior of *Lr*PduO with Cbl bound in the base-off−His-on conformation and discuss possible reasons why ACA enzymes do not bind Cbl in the His-on form.

EXPERIMENTAL PROCEDURES

Protein Production and Purification. Variants of *Lr*PduO were generated using the QuickChange XL site-directed mutagenesis kit (Stratagene). The pTEV3 plasmid (*22*) carrying the wild-type *Lr* $pduO^+$ allele (*23*) was used as a template for polymerase chain reaction (PCR)-based site-directed mutagenesis as per the manufacturer's instructions. The presence and nature of the mutations were verified by sequencing the plasmids using nonradioactive BigDye (ABI-PRISM) protocols. Sequencing reactions were resolved at the DNA sequence facility of the Biotechnology Center of the University of Wisconsin. Recombinant *Lr*PduO variants were overexpressed in *Escherichia coli* strain BL21 (DE3). Derivatives of plasmid pTEV3 carrying *Lr pduO* alleles encoding *Lr*PduO variants with a rTEV protease-cleavable N-terminal His_6 tag were constructed, genes overexpressed, and proteins isolated using Ni^{2+} affinity chromatography as described elsewhere (*23*); N-terminal tags were cleaved using rTEV protease (*24*). Flavodoxin (FldA) and ferredoxin (flavodoxin):$NADP^+$ reductase (Fpr) were produced and purified as described previously (*25, 26*).

*Crystallization and Data Collection. Lr*PduO variant proteins were produced and purified using described protocols (*23*). All crystals of tag-less *Lr*PduO proteins were grown using the vapor diffusion method in an anoxic chamber at 25 °C. The protein concentration in the crystallization solutions was 12, 15, and 11 mg/mL for the *Lr*$PduO^{F112A}$, *Lr*$PduO^{F112H}$, and *Lr*$PduO^{\Delta183}$ variants, respectively. Crystals of the precatalytic Cbl complex for the *Lr*$PduO^{F112A}$ variant [*Lr*$PduO^{F112A}$−ATP:cob(II)alamin] were grown by mixing 3.5 μL of a protein solution containing *E. coli* FMN reductase (Fre; 30 μg/mL), NADH (50 mM), FMN (10 mM), HOCbl (10 mM), ATP (10 mM), $MgCl_2$ (10 mM), and NaCl (300 mM) with 3.5 μL of a reservoir solution {polyethylene glycol (PEG) 8000 [14% (w/v)], KCl (200 mM), and 2-(*N*-morpholino)ethanesulfonic acid (MES, 100 mM, pH 6)}. Crystals of the precatalytic Cbl complex for the *Lr*$PduO^{\Delta183-188}$ protein were grown by mixing 3.5 μL of a protein solution containing Fre (30 μg/mL), NADH (10 mM), FMN (2 mM), HOCbl (2 mM), ATP (2.5 mM), $MgCl_2$ (2.5 mM), and NaCl (300 mM) with 3.5 μL of a reservoir solution {PEG 8000 [14% (w/v)], KCl (200 mM), and MES (100 mM, pH 6)}. Crystals of the precatalytic Cbl complex for the *Lr*$PduO^{F112H}$ protein were grown by mixing 3.5 μL of a protein solution containing Fre (30 μg/mL), NADH (10 mM), FMN (2 mM), HOCbl (2 mM), ATP (2.5 mM), $MgCl_2$ (2.5 mM), and NaCl (300 mM) with 3.5 μL of a reservoir solution {PEG 8000 [14% (w/v)], KCl (200 mM), 3-[4-(2-hydroxyethyl)piperazin-1-yl]propane-1-sulfonic acid (HEPPS, 100 mM, pH 8.6)}. Several large, brown-colored, cubic crystals (~200 μm^3) appeared spontaneously after 24 h and were grown for an additional 48 h. The crystals for each of the *Lr*PduO proteins were transferred to an anoxic synthetic mother liquor solution {glycerol [2% (v/v)] and PEG 8000 [10% (w/v)]}, MES (100 mM, pH 6), or, for *Lr*$PduO^{F112H}$, HEPPS (100 mM, pH 8.6), KCl (200 mM), Fre (35 μg/mL), NADH (10 mM), FMN (2 mM), HOCbl (2 mM), ATP (2 mM), $MgCl_2$ (2.5 mM) and, in an anoxic chamber, incrementally transferred in five steps to an anoxic cryoprotectant solution {glycerol [20% (v/v)], PEG 8000 [12% (w/v)], MES (100 mM, pH 6), or, for *Lr*$PduO^{F112H}$, HEPPS (100 mM, pH 8.6), KCl (300 mM), Fre (35 μg/mL), NADH (10 mM), FMN (2 mM), HOCbl (2 mM), ATP (2 mM), and $MgCl_2$ (2.5 mM)}. The crystals were briefly exposed to oxygen (≤5 s) while they were flash-frozen in liquid nitrogen.

All crystals belong to space group *R*3 with one subunit in the asymmetric unit. Data sets were collected at the Advanced Photon Source in Argonne, IL, on beamline 19BM. Diffraction data were integrated and scaled with *HKL2000* (*27*). Data collection statistics are summarized in Table 1.

Structure Determination and Refinement. The structures were determined by molecular replacement with MOLREP (*28*) starting from the model of the wild-type *Lr*PduO protein in complex with ATP (PDB entry 2NT8). Final refinement was carried out with REFMAC (*29*). Heteroatoms, water molecules, and multiple conformations were built using COOT (*30*). The final *Lr*$PduO^{F112A}$−ATP:cob(II)alamin, *Lr*$PduO^{F112H}$−ATP:cob(II)alamin, and *Lr*$PduO^{\Delta183-188}$−ATP:cob(II)alamin models were refined to 1.5, 1.2, and 1.4, respectively. The models include residues 2−182, 1−188, and 2−181 for *Lr*$PduO^{F112A}$, *Lr*$PduO^{F112H}$, and *Lr*$PduO^{\Delta183}$, respectively. Ramachandran plots for all models show that >96% of residues are in the most favored region with no residues falling in the disallowed region. Refinement statistics are listed in Table 1.

In Vitro Adenosylation Activity Assays. The Co^+ assays were performed using the continuous spectrophotometric method described previously, without modifications (*23*). In this assay, the cobalt ion of Cbl is chemically reduced in solution to cob(I)alamin by Ti(III)citrate. The Co^+ assay was performed under anoxic conditions, and the adenosylation reaction was initiated by the addition of *Lr*PduO. The reaction mixture included 2-amino-2-hydroxymethylpropane-1,3-diol hydrochloride (Tris-HCl, 0.2 M; pH 8 at 37 °C), $MgCl_2$ (1.5 mM), HOCbl (0.1−20 μM), and ATP (1 μM to 1 mM). The Co^{2+} assay was modified from a previously used end-point assay (*26*) to allow the appearance of product (AdoCbl) to be continuously monitored in the presence of a protein reducing system. The Co^{2+} assays were performed under anoxic conditions at 37 °C. Empty quartz cuvettes were

Table 1: Data Collection and Refinement Statistics[a]

	*Lr*PduO^{F112A}	*Lr*PduO^{F112H}	*Lr*PduO$^{\Delta183}$
space group	*R*3	*R*3	*R*3
cell dimensions			
a, *b*, *c* (Å)	80.7, 80.7, 89.7	80.9, 80.9, 90.0	67.7, 67.7, 111.2
α, *β*, *γ* (deg)	90, 90, 120	90, 90, 120	90, 90, 120
resolution range (Å)	30.0−1.48 (1.52−1.48)	30.0−1.17 (1.20−1.17)	30.0−1.38 (1.43−1.38)
redundancy	5.6 (5.0)	4.4 (2.0)	6.3 (3.1)
completeness (%)	99.7 (98.6)	99.6 (97.3)	97.3 (82.0)
no. of unique reflections	36186	73398	38038
R_{merge} (%)	5.7 (12.8)	7.0 (17.9)	6.3 (9.7)
average I/σ	46.2 (13.4)	41.4 (6.2)	47.7 (14.3)
R_{cryst}	0.156 (0.150)	0.161 (0.202)	0.162 (0.154)
R_{free}	0.174 (0.172)	0.182 (0.203)	0.181 (0.169)
no. of protein atoms	1543	1619	1517
no. of water molecules	158	211	167
Wilson *B* value (Å^2)	23.4	15.1	14.3
average *B* factor (Å^2)			
protein	17.8	13.4	12.9
ligands	20.0	14.7	14.9
solvent	32.3	29.0	26.9
Ramachandran (%)			
most favored	96.4	96.5	97.6
additionally allowed	3.6	3.5	2.4
generously allowed	0	0	0
disallowed	0	0	0
root-mean-square deviation			
bond lengths (Å)	0.014	0.022	0.012
bond angles (deg)	2.20	2.85	2.09

[a] Values in parentheses are for the highest-resolution bin.

flushed with oxygen-free N_2 for 5 min. Under a stream of O_2-free N_2, 2-amino-2-hydroxymethylpropane-1,3-diol hydrochloride (Tris-HCl, 0.2 M; pH 8 at 37 °C), KCl (0.1 M), $MgCl_2$ (1.5 mM), HOCbl (4 μM to 0.2 mM), Fpr (73 μg/mL), FldA (0.6 mg/mL), NADPH (1 mM), and ATP (1 μM to 1 mM) were added to the cuvette in the order stated. To ensure that all cob(III)alamin was reduced to cob(II)alamin, reaction mixtures were incubated at 37 °C for 10 min. The adenosylation reaction was initiated by the addition of the *Lr*PduO protein. The appearance of AdoCbl was monitored at 525 nm. To minimize the contribution from photolysis, initial velocities were measured within the first 5 min after reaction was initiated. The photolysis of AdoCbl at 525 nm over the first 5 min was determined to be insignificant (data not shown). The reduction of cob(II)alamin was monitored at 473 nm using the Co^{2+} assay.

In Vivo Assessment of Function. The function of *Lr*PduO proteins was also assessed in vivo. For this purpose, we used a strain of *Salmonella enterica* serovar Typhimurium LT2 that carried a chromosomal deletion of the *cobA* gene that encodes the housekeeping ATP:Co(I)rrinoid adenosyltransferase. CobA is needed for salvaging cobinamide (Cbi), a precursor of AdoCbl (*31, 32*). As shown elsewhere, the *Lr pduO*$^+$ gene substitutes for the *cobA*$^+$ gene during growth of a *cobA* strain on minimal medium supplemented with glycerol (30 mM) and dicyano-Cbi [$(CN)_2$Cbi, 150 nM] (*23, 33*).

RESULTS AND DISCUSSION

Spectroscopic and structural analyses have shown that PduO-type ACA enzymes facilitate the thermodynamically unfavorable Co^{2+} to Co^+ reduction of the cobalt ion in corrinoids by generating a four-coordinate Co(II) corrinoid species with no axial (α and *β*) ligands (*17, 18*). To gain insights into the molecular basis of the formation of the four-coordinate Co(II) corrinoid species in PduO-type ACA enzymes, we performed structural and kinetic analysis of *Lr*PduO enzyme variants.

We used two assays to distinguish between the two functions of *Lr*PduO, namely, assistance in the reduction of Co^{2+} to Co^+ and Co(I) corrinoid adenosylation. In one assay, we used the NADPH-dependent flavodoxin protein reductase (Fpr)/flavodoxin (FldA) system to reduce Co^{2+} to Co^+; hereafter, this assay is termed the Co^{2+} assay. In the Co^{2+} assay, the PduO enzyme must bind cob(II)alamin and facilitate the generation of cob(I)alamin in its active site. Conversely, in the second assay, termed the Co^+ assay, we used Ti(III)citrate to reduce Co^{2+} to Co^+ in solution, allowing the cob(I)alamin adenosylation reaction to be measured directly. Cobalamin was used as the corrinoid substrate in both assays. The Co^{2+} assay allowed us to indirectly assess the formation of the four-coordinate cob(II)alamin species, whereas the Co^+ assay allowed us to assess the catalytic competency of the variants. We used both assays in combination with high-resolution crystal structures to identify residues involved in the formation of the four-coordinate cob(II)alamin species.

Residue Phe112 Displaces the Lower Ligand. The crystal structure of *Lr*PduO in complex with cob(II)alamin and ATP revealed cob(II)alamin bound in a conformation with the lower axial ligand (DMB) excluded from the active site (*21*) (Figure 1A). Residue Phe112 is positioned 3.8 Å from the cobalt ion, suggesting that this residue plays an important role in the formation of the four-coordinate cob(II)alamin intermediate (*21, 34, 35*). To further investigate the role of Phe112, we changed the coding sequence of the *Lr pduO*$^+$ gene to encode variant protein *Lr*PduO^{F112A}. The latter was crystallized under anoxic conditions, and its X-ray structure was determined at 1.5 Å resolution. The crystal structure of *Lr*PduO^{F112A} revealed cob(II)alamin bound to the active site as a five-coordinate

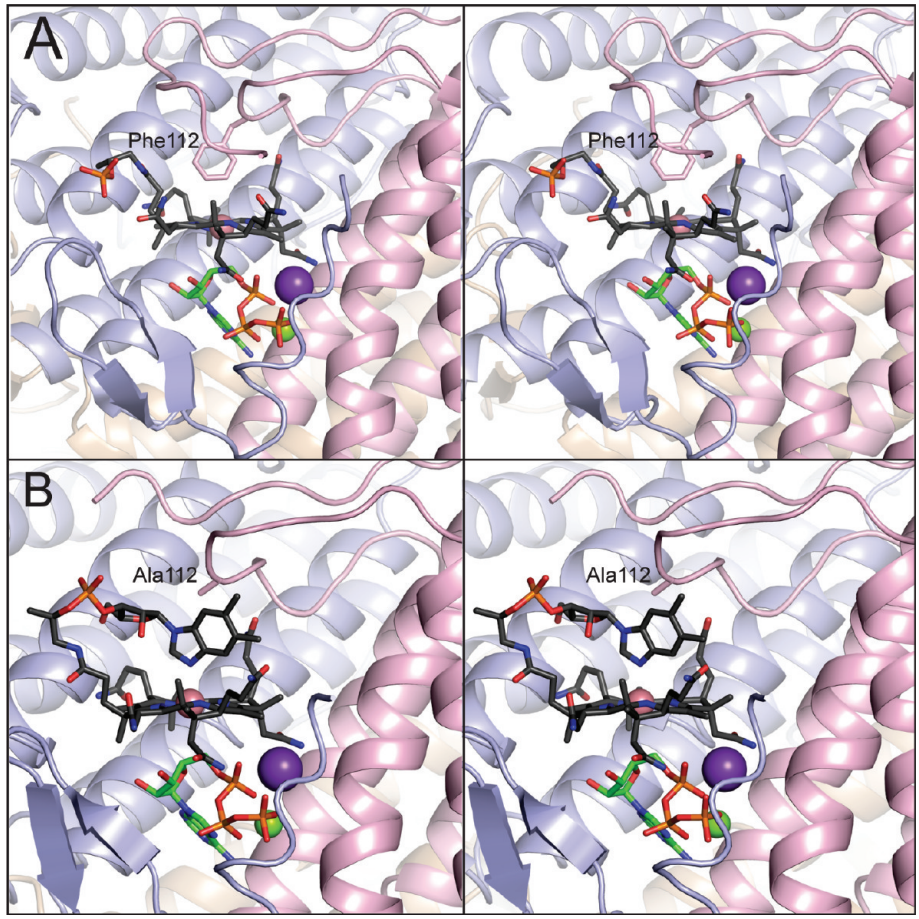

FIGURE 1: Phe112 displaces the lower ligand of cob(II)alamin in *Lr*PduO to generate a four-coordinate intermediate. Stereoviews of the active sites of (A) wild-type *Lr*PduO [PDB entry 3CI1 (*21*)] and (B) *Lr*PduO^{F112A} with the individual subunits of the trimer represented as ribbons colored blue, red, and brown. For the sake of clarity, only the active site at the interface of the red and blue subunits is shown. The carbon atoms of cob(II)alamin are colored black, while the carbon atoms of ATP are colored green. The potassium (purple sphere) and magnesium (green sphere) atoms are also displayed. The electron density corresponding to the DMB portion of cob(II)alamin is disordered in the wild-type structure.

Table 2: Kinetic Parameters of *Lr*PduO Variants Using the Co^+ Assay[a]

	ATP			cob(I)alamin		
enzyme	K_m (μM)	k_{cat} (s^{-1})	k_{cat}/K_m (M^{-1} s^{-1})	K_m (μM)	k_{cat} (s^{-1})	k_{cat}/K_m (M^{-1} s^{-1})
wild type	2.2 ± 0.1	$(2.6 \pm 0.1) \times 10^{-2}$	$(1.2 \pm 0.1) \times 10^4$	0.13 ± 0.01	$(2.4 \pm 0.1) \times 10^{-2}$	$(1.8 \pm 0.2) \times 10^5$
F112A	34.6 ± 8.8	$(5.6 \pm 0.0) \times 10^{-3}$	$(1.7 \pm 0.4) \times 10^2$	1.9 ± 0.5	$(6.6 \pm 0.5) \times 10^{-3}$	$(3.6 \pm 1.0) \times 10^3$
F112H	2.6 ± 0.0	$(3.8 \pm 0.1) \times 10^{-4}$	$(1.4 \pm 0.1) \times 10^2$	2.8 ± 0.4	$(4.2 \pm 0.1) \times 10^{-4}$	$(1.5 \pm 0.2) \times 10^2$
F112Y	1.2 ± 0.1	$(1.6 \pm 0.0) \times 10^{-3}$	$(1.4 \pm 0.1) \times 10^3$	0.55 ± 0.05	$(1.7 \pm 0.0) \times 10^{-3}$	$(3.1 \pm 0.3) \times 10^3$
F112W	2.0 ± 0.6	$(1.8 \pm 0.2) \times 10^{-3}$	$(9.8 \pm 3.4) \times 10^2$	0.77 ± 0.12	$(2.0 \pm 0.2) \times 10^{-3}$	$(2.6 \pm 0.5) \times 10^3$
F163A	15.9 ± 6.8	$(1.5 \pm 0.1) \times 10^{-2}$	$(1.8 \pm 0.4) \times 10^3$	0.19 ± 0.03	$(1.5 \pm 0.3) \times 10^{-2}$	$(7.9 \pm 1.9) \times 10^4$
F187A	1.2 ± 0.4	$(2.1 \pm 0.4) \times 10^{-2}$	$(1.7 \pm 0.6) \times 10^4$	0.11 ± 0.01	$(1.8 \pm 0.1) \times 10^{-2}$	$(1.6 \pm 0.2) \times 10^5$
ΔS183	3.1 ± 0.2	$(2.3 \pm 0.6) \times 10^{-2}$	$(7.5 \pm 2.2) \times 10^3$	0.07 ± 0.06[b]	$(2.0 \pm 0.2) \times 10^{-2}$	3.95×10^5

[a] The substrate cob(I)alamin was generated chemically using Ti(III)citrate. [b] Significant error due to absorbance near the detection limit.

species with DMB serving as a fifth axial ligand (Figure 1B). The *Lr*PduO^{F112A} variant displayed extremely low activity in the Co^{2+} assay. However, in the Co^+ assay [adenosylation of cob(I)alamin], *Lr*PduO^{F112A} was catalytically competent and displayed only a slight decrease in k_{cat} (~4-fold) (Table 2). This result is consistent with the idea that, in the absence of a four-coordinate cob(II)alamin species, the enzyme is inactive. The kinetic parameters of the *Lr*PduO^{F112A} enzyme support the idea that the steric bulk presented by the phenyl moiety of the side chain of Phe112 is critical for the formation of the four-coordinate species and hence to the reactivity of the enzyme.

Effects of an F112H Substitution. Several Cbl-dependent enzymes share the Cbl-binding motif "**DXHXXG**", in which the histidinyl residue coordinates to the cobalt ion (*36*) generating a DMB-off/His-on conformation of the cofactor (*12, 37*); the **DXHXXG** motif is not present in any ACA enzyme. The proximity of residue Phe112 to the cobalt ion of Cbl offered an opportunity to generate a DMB-off/His-on ACA enzyme by site-directed mutagenesis, allowing us to assess the effect of a DMB-off/His-on complex on the activity of the enzyme. The *Lr*PduO^{F112H} variant was constructed, and its X-ray crystal structure was determined to 1.5 Å resolution. The structure of *Lr*PduO^{F112H} confirmed that cob(II)alamin was bound in a DMB-off/His-on conformation (Figure 2). The F112H substitution resulted in a substantial drop in k_{cat} (~60-fold) in assays Co^{2+} and Co^+ (Tables 2 and 3), suggesting that *Lr*PduO^{F112H} was impaired

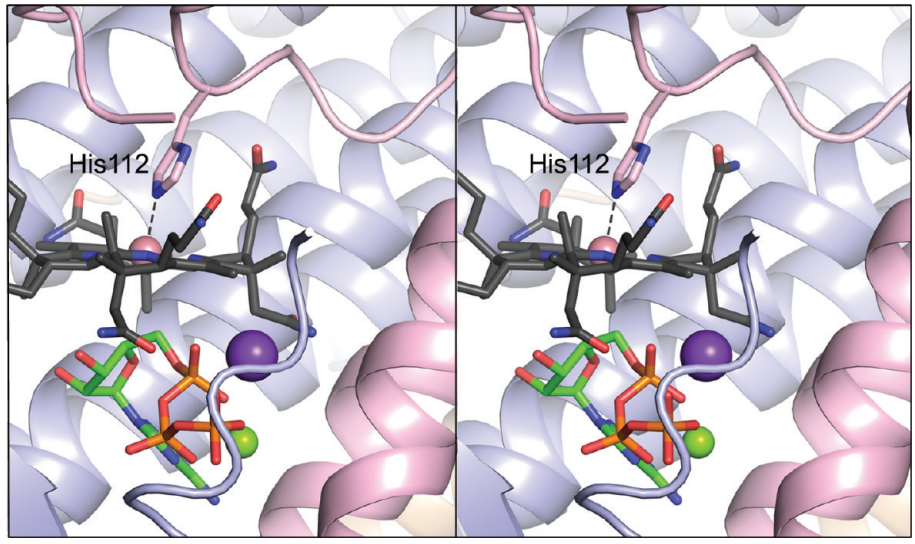

FIGURE 2: His112 acts as a lower ligand to five-coordinate cob(II)alamin in *Lr*PduO^{F112H}. Stereoview of *Lr*PduO^{F112H} with the individual subunits of the trimer represented as ribbons colored blue, red, and brown. For the sake of clarity, only the active site at the interface of the red and blue subunits is shown. The carbon atoms of cob(II)alamin are colored black, while the carbon atoms of ATP are colored green. The potassium (purple sphere) and magnesium (green sphere) atoms are also displayed. The electron density corresponding to the DMB portion of cob(II)alamin is disordered, and therefore, DMB could not be modeled.

Table 3: Kinetic Parameters of Wild-Type *Lr*PduO and Variants Using the Co^{2+} Assay[a]

	ATP			cob(II)alamin		
enzyme	K_m (μM)	k_{cat} (s^{-1})	k_{cat}/K_m (M^{-1} s^{-1})	K_m (μM)	k_{cat} (s^{-1})	k_{cat}/K_m (M^{-1} s^{-1})
wild type	5.5 ± 1.1	$(2.9 \pm 0.1) \times 10^{-2}$	$(5.5 \pm 1.1) \times 10^{3}$	7.8 ± 1.1	$(3.8 \pm 0.5) \times 10^{-2}$	$(4.8 \pm 0.9) \times 10^{3}$
F112A	UD[b]	UD[b]		UD[b]	UD[b]	
F112H	10.4 ± 0.8	$(5.9 \pm 0.2) \times 10^{-4}$	$(5.7 \pm 0.5) \times 10$	53.0 ± 8.6	$(6.7 \pm 0.2) \times 10^{-4}$	$(1.3 \pm 0.2) \times 10^{1}$
F112Y	9.4 ± 0.4	$(2.3 \pm 0.1) \times 10^{-3}$	$(2.5 \pm 0.2) \times 10^{2}$	34.2 ± 10.7	$(2.7 \pm 0.4) \times 10^{-3}$	$(8.3 \pm 2.8) \times 10^{1}$
F112W	7.3 ± 0.1	$(2.8 \pm 0.1) \times 10^{-3}$	$(3.9 \pm 0.2) \times 10^{2}$	28.8 ± 5.7	$(3.2 \pm 0.1) \times 10^{-3}$	$(1.1 \pm 0.2) \times 10^{2}$
F163A	96.1 ± 7.1[c]	$(1.5 \pm 0.1) \times 10^{-2}$[b]	$(1.6 \pm 0.2) \times 10^{2}$[b]	134 ± 13	$(2.7 \pm 0.4) \times 10^{-2}$	$(2.0 \pm 0.3) \times 10^{2}$
F187A	7.9 ± 1.0	$(1.4 \pm 0.1) \times 10^{-2}$	$(1.8 \pm 0.3) \times 10^{3}$	15.8 ± 3	$(1.5 \pm 0.1) \times 10^{-2}$	$(9.3 \pm 1.9) \times 10^{2}$
ΔS183	9.9 ± 0.9	$(1.7 \pm 0.1) \times 10^{-2}$	$(1.7 \pm 0.2) \times 10^{3}$	16.3 ± 1.7	$(1.8 \pm 0.1) \times 10^{-2}$	$(1.1 \pm 0.1) \times 10^{3}$

[a] The substrate cob(II)alamin was generated using a protein reducing system. The saturating level of ATP was at least 100-fold greater than the K_M; however, the saturating level of cob(II)alamin was limited to being 3−10-fold greater than the K_M as a result of assay sensitivity. [b] Unable to determine constants due to extremely low activity. [c] Kinetic parameters obtained at subsaturating concentrations of cob(II)alamin.

in its ability to catalyze the adenosylation of cob(I)alamin and/or release the AdoCbl product. Notably, the specific activity of *Lr*PduO^{F112H} for the reduction of cob(II)alamin to cob(I)alamin was only 19-fold lower than that of the wild-type *Lr*PduO protein (1.5 and 28 mM Co^{1+} min^{-1} mg^{-1}, respectively).

We also measured an ~5 min lag in the reduction of cob(II)alamin (Co^{2+} assay), but not in the adenosylation reaction (Co^{+} assay); the observed lag did not depend on the concentration of the reagents or substrates (data not shown). Overlays of spectral scans (from 300 to 700 nm) obtained at different times showed a lag in the generation of product (i.e., AdoCbl; 525 nm), but not in the reduction of the substrate (Figure 3). Since the Co^{2+} assay is essentially a coupled assay (i.e., reduction followed by adenosylation), the observed lag is consistent with cob(I)alamin adenosylation being the rate-limiting step in the reaction catalyzed by *Lr*PduO^{F112H}. Reaction lags are typically observed in coupled assays where the second step in the reaction is rate-limiting (*38*).

The Severity of the Effect of Different α *Ligands on LrPduO Activity Varies Substantially.* Even though *Lr*PduO^{F112A} and *Lr*PduO^{F112H} proteins bound cob(II)alamin as a five-coordinate species (Figures 1B and 2), their enzymatic activity was vastly different. The critical distinction between these two variants lies in the nature of the α ligand. In *Lr*PduO^{F112H}, the α ligand is a histidinyl side chain of the enzyme, whereas in *Lr*PduO^{F112A}, the α ligand is DMB. The explanation for the kinetic differences is not immediately obvious since the Co−N coordination bond in both variants is very similar in the crystal structures. The apparent similarity, however, may be imposed by the packing in the crystals. Indeed, recent spectroscopic analysis of these variants revealed the coordination bond between Co and N(His^{112}) to be longer than the bond between Co and N(DMB) (K. Park et al., manuscript in preparation). A longer Co−N(His^{112}) coordination bond in *Lr*PduO^{F112H} would result in a faster displacement of the lower ligand, and therefore a higher k_{cat} in the Co^{2+} assay.

To explain the data shown in Figure 3, we propose that the reduced k_{cat} of *Lr*PduO^{F112H} may be the result of a slower nucleophilic attack by the Co ion of cob(I)alamin on the 5′-carbon of ATP, and/or a slow product release. Considering that the Co−C bond in AdoCbl is formed with cob(I)alamin (a four-coordinate Cbl species), wild-type *Lr*PduO may first generate an AdoCbl/DMB-off product, a cob(III)alamin species that is energetically unstable in the absence of an α axial ligand. Consequently, a DMB-on conformation would be favored prior to, or concomitant with, product release. In *Lr*PduO^{F112H}, the coordination bond with N(His) may sta-

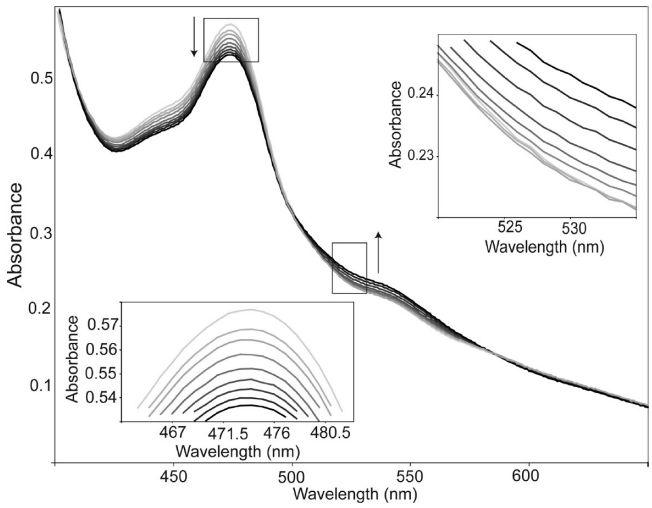

FIGURE 3: Spectral changes associated with the enzymic conversion of cob(II)alamin to AdoCbl by *Lr*PduO^{F112H}. Arrows and increasing darkness in the spectra represent successive time points after reaction was initiated by the addition of ATP (light gray, 1 min; black, 11 min). *Lr*PduO^{F112H} facilitates the reduction of cob(II)alamin (as evidenced by the decrease in absorbance at 473 nm); however, there is a lag in the generation of AdoCbl (as evidenced in initial lag in absorbance at 525 nm).

bilize Co^{3+} of AdoCbl, resulting in an AdoCbl/His-on species. For product to be released, AdoCbl/His-on must first undergo the thermodynamically unfavorable step that generates AdoCbl/DMB-off. This scenario would be consistent with a slow product release step and would explain the equivalent drop in the k_{cat} of *Lr*PduO^{F112H} with cob(I)alamin and cob(II)alamin relative to that of the wild-type enzyme. Similarly, other Phe112 variants (i.e., *Lr*PduO^{F112Y} and *Lr*PduO^{F112W}) retained their ability to adenosylate cob(I-I)alamin, albeit not as efficiently as the wild-type protein (Table 3). The k_{cat} values of variants *Lr*PduO^{F112W} and *Lr*PduO^{F112Y} decreased ~10-fold in both assays, suggesting a problem with product realease like the one observed with *Lr*PduO^{F112H}. This is possible since Trp112 and Tyr112 have functional groups that can interact with the cobalt ion of Cbl.

In contrast with ACA enzymes, Cbl-dependent enzymes that bind Cbl in its base-off/His-on form would not have the problem of product release because Cbl stays bound to the enzyme acting as a radical initiator or methyl carrier. In PduO-type enzymes, phenylalanine is the ideal residue for PduO-type enzymes because it is bulky enough to displace the lower ligand of Cbl and does not coordinate with the cobalt ion of Cbl; hence, product release can be rapid. Further studies of product release in wild-type *Lr*PduO and *Lr*PduO^{F112H} proteins are needed to improve our understanding of the effect of the Co−N(His) coordination in *Lr*PduO^{F112H}.

Function of Other Hydrophobic Residues in the Cbl-Binding Site of LrPduO. The structure of *Lr*PduO in complex with ATP and cob(II)alamin shows a hydrophobic pocket with aromatic residues around the corrin ring. In hemoproteins, interactions between heme and aromatic side chains have been proposed to stabilize the holoprotein fold and to contribute to the high affinity of the protein for heme (*39*). To determine whether additional aromatic residues play a role in PduO-mediated catalysis, two phenylalanine residues, Phe163 and Phe187, located inside the hydrophobic pocket were changed by site-directed mutagenesis.

(i) Phe163. Residue Phe163 is conserved in all PduO-type enzymes, except in *S. enterica* PduO, where tyrosine occupies this position. The structurally equivalent residue in the human ACA enzyme was suggested to be involved in Cbl binding (*34, 35*). Notably, the K_m of *Lr*PduO^{F163A} for cob(II)alamin increased significantly (17-fold), but the k_{cat} remained unchanged (Table 3). In contrast, the K_m and the k_{cat} of *Lr*PduO^{F163A} for cob(I)alamin were very similar to those of the wild-type enzyme (Table 2). Together, these results suggest that Phe163 and DMB interact when Cbl binds to the active site of *Lr*PduO. The negative effect of the substitution is not observed with cob(I)alamin because this form of Cbl does not have the axial ligands.

(ii) Phe187. Although residue Phe187 is not conserved, it is part of the C-terminal loop (Ser183−Arg188) that becomes ordered upon binding of the corrinoid substrate (*21*). The kinetic parameters of *Lr*PduO^{F187A} for cob(I)alamin and cob(II)alamin were not significantly different from the parameters of the wild-type enzyme (Tables 2 and 3).

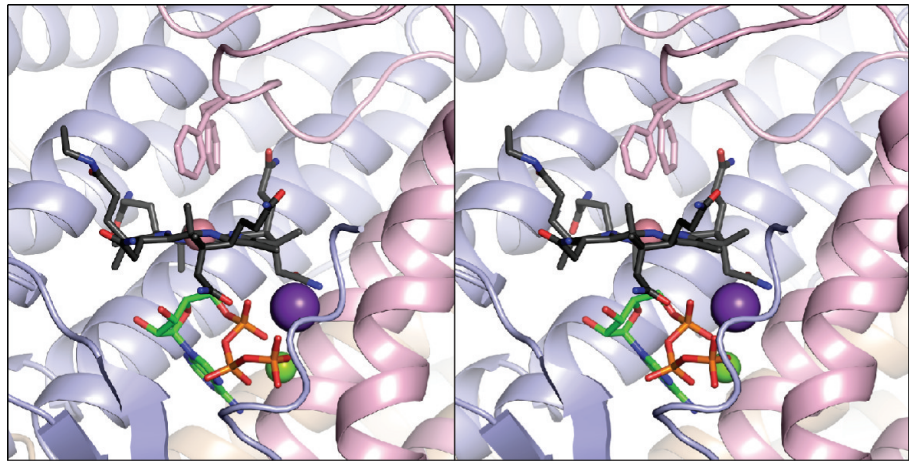

FIGURE 4: *Lr*PduO$^{\Delta 183}$ variant retains the ability to generate a four-coordinate intermediate. Stereoview of *Lr*PduO$^{\Delta 183}$ with the individual subunits of the trimer represented as ribbons colored blue, red, and brown. For the sake of clarity, only the active site at the interface of the red and blue subunits is shown. The carbon atoms of cob(II)alamin are colored black, while the carbon atoms of ATP are colored green. The potassium (purple sphere) and magnesium (green sphere) atoms are also displayed. Residue Phe112 adopts two alternate conformations in this structure. Both conformations are displayed. The electron density corresponding to the DMB portion of cob(II)alamin is disordered, and therefore, DMB could not be modeled.

To analyze the contribution of the C-terminal loop to the function of *Lr*PduO, we deleted the last six amino acid residues of the protein (i.e., Ser183−Arg188). The crystal structure of the *Lr*PduO$^{\Delta 183-188}$ protein was determined to 1.4 Å resolution (Figure 4). The absence of the C-terminal residues resulted in greater conformational freedom for residue Phe112 in the active site, with the electron density suggesting two alternative conformations for the side chain of Phe112. The crystal structure of the *Lr*PduO$^{\Delta 183-188}$ protein also showed that a four-coordinate cob(II)alamin intermediate could still form in the active site of the enzyme (Figure 4). Consistent with this finding, the catalytic efficiency of the *Lr*PduO$^{\Delta 183-188}$ protein was only modestly reduced (3−4-fold) (Tables 2 and 3), suggesting that the C-terminus of the proteins can be modified or truncated without there being a profound impact on the catalytic efficiency of the enzyme.

In Vivo Functionality of LrPduO Variants. None of the variants, even those with measurable activity, supported AdoCbl biosynthesis in vivo (data not shown). The fact that the *Lr*PduO$^{\Delta 183-188}$ protein did not support in vivo biosynthesis of AdoCbl, in spite of its modest decrease in activity, suggests that this part of the protein may be important for protein−protein interactions. ATP corrinoid adenosyltransferases are thought to transport this valuble but limited coenzyme to the corresponding AdoCbl-dependent enzyme (*40*). In the human adenosyltransferase, a truncation of the final 16 residues has been shown to result in an early onset of methylmalonic aciduria (*41*).

CONCLUSIONS

Here we report structural and kinetic data to support the idea that the inability to generate the four-coordinate cob(II)alamin intermediate renders a human-type ACA enzyme inactive. The side chain of residue Phe112 in the active site of the enzyme is critical to the function of the enzyme for three reasons. (i) It is in the proximity of the Co ion of the ring. (ii) It is bulky. (iii) It cannot form a coordination bond with the Co ion. Hence, when cob(II)alamin binds to the enzyme, the lower ligand is displaced and the resulting four-coordinate cob(II)alamin species remains as such because the phenyl side chain cannot form a coordination bond with the Co ion.

ACKNOWLEDGMENT

We thank Thomas Brunold and Kiyoung Park (Department of Chemistry, University of Wisconsin) for helpful discussions and critical review of the manuscript. Structural Biology BM19 beamline at the Argonne National Laboratory Advanced Photon Source was supported by the U.S. Department of Energy, Office of Energy Research, under Contract W-31-109-ENG-38.

REFERENCES

1. Halpern, J. (1985) Mechanisms of coenzyme B_{12}-dependent rearrangements. *Science 227*, 869–875.
2. Banerjee, R., and Chowdhury, S. (1999) Methylmalonyl-CoA mutase. In *Chemistry and Biochemistry of B12* (Banerjee, R., Ed.) pp 707−729, John Wiley & Sons, Inc., New York.
3. Buckel, W., Bröker, G., Bothe, H., and Pierik, A. (1999) Glutamate mutase and 2-Methylglutarate mutase. In *Chemistry and Biochemistry of B12* (Banerjee, R., Ed.) pp 757−782, John Wiley & Sons, Inc., New York.
4. Bandarian, V., and Reed, G. H. (1999) Ethanolamine ammonia-lyase. In *Chemistry ad Biochemistry of B12* (Banerjee, R., Ed.) pp 811−833, John Wiley & Sons, Inc., New York.
5. Toraya, T. (1999) Diol dehydratase and glycerol dehydratase. In *Chemistry and Biochemistry of B12* (Banerjee, R., Ed.) pp 783−809, John Wiley & Sons, Inc., New York.
6. Fontecave, M. (1998) Ribonucleotide reductases and radical reactions. *Cell. Mol. Life Sci. 54*, 684–695.
7. Fontecave, M., and Mulliez, E. (1999) Ribonucleotide Reductases. In *Chemistry and Biochemistry of B12* (Banerjee, R., Ed.) pp 731−756, John Wiley & Sons, Inc., New York.
8. Wohlfarth, G., and Diekert, G. (1999) Reductive dehalogenases. In *Chemistry and Biochemistry of B12* (Banerjee, R., Ed.) pp 871−893, John Wiley & Sons, Inc., New York.
9. Gärtner, P., Ecker, A., Fischer, R., Linder, D., Fuchs, G., and Thauer, R. K. (1993) Purification and properties of N5-methyltetrahydromethanopterin:coenzyme M methyltransferase from *Methanobacterium thermoautotrophicum*. *Eur. J. Biochem. 213*, 537–545.
10. Taylor, R. T., and Weissbach, H. (1973) N5-Methylenetetrahydrofolate-homocysteine methyltransferases. In *The Enzymes* (Boyer, P. D., Ed.) pp 121−165, Academic Press, Inc., New York.
11. van der Meijden, P., Brommelstroet, B. W. t., Poiroit, C. M., van der Drift, C., and Vogels, G. D. (1984) Purification and properties of methanol:5-hydroxybenzimidazolylcobamide methyltransferase from *Methanosarcina barkeri*. *J. Bacteriol. 160*, 629–635.
12. Mancia, F., Keep, N. H., Nakagawa, A., Leadlay, P. F., McSweeney, S., Rasmussen, B., Bosecke, P., Diat, O., and Evans, P. R. (1996) How coenzyme B12 radicals are generated: The crystal structure of methylmalonyl-coenzyme A mutase at 2 Å resolution. *Structure 4*, 339–350.
13. Drennan, C. L., Huang, S., Drummond, J. T., Matthews, R. G., and Ludwig, M. L. (1994) How a protein binds B_{12}: A 3.0Å X-ray structure of B_{12}-binding domains of methionine synthase. *Science 266*, 1669–1674.
14. Fonseca, M. V., and Escalante-Semerena, J. C. (2000) Reduction of cob(III)alamin to cob(II)alamin in *Salmonella enterica* Serovar Typhimurium LT2. *J. Bacteriol. 182*, 4304–4309.
15. McIver, L., Leadbeater, C., Campopiano, D. J., Baxter, R. L., Daff, S. N., Chapman, S. K., and Munro, A. W. (1998) Characterisation of flavodoxin $NADP^+$ oxidoreductase and flavodoxin: Key components of electron transfer in *Escherichia coli*. *Eur. J. Biochem. 257*, 577–585.
16. Olteanu, H., Wolthers, K. R., Munro, A. W., Scrutton, N. S., and Banerjee, R. (2004) Kinetic and thermodynamic characterization of the common polymorphic variants of human methionine synthase reductase. *Biochemistry 43*, 1988–1997.
17. Stich, T. A., Yamanishi, M., Banerjee, R., and Brunold, T. C. (2005) Spectroscopic evidence for the formation of a four-coordinate Co^{2+}cobalamin species upon binding to the human ATP: cobalamin adenosyltransferase. *J. Am. Chem. Soc. 127*, 7660–7661.
18. Stich, T. A., Buan, N. R., Escalante-Semerena, J. C., and Brunold, T. C. (2005) Spectroscopic and computational studies of the ATP: Corrinoid adenosyltransferase (CobA) from *Salmonella enterica*: Insights into the mechanism of adenosylcobalamin biosynthesis. *J. Am. Chem. Soc. 127*, 8710–8719.
19. Park, K., Mera, P. E., Escalante-Semerena, J. C., and Brunold, T. C. (2008) Kinetic and spectroscopic studies of the ATP:corrinoid adenosyltransferase PduO from *Lactobacillus reuteri*: Substrate specificity and insights into the mechanism of Co(II)corrinoid reduction. *Biochemistry 47*, 9007–9015.
20. Yamanishi, M., Labunska, T., and Banerjee, R. (2005) Mirror "base-off" conformation of coenzyme B12 in human adenosyltransferase and its downstream target, methylmalonyl-CoA mutase. *J. Am. Chem. Soc. 127*, 526–527.
21. St Maurice, M., Mera, P., Park, K., Brunold, T. C., Escalante-Semerena, J. C., and Rayment, I. (2008) Structural characterization of a human-type corrinoid adenosyltransferase confirms that coenzyme B12 is synthesized through a four-coordinate intermediate. *Biochemistry 47*, 5755–5766.
22. Rocco, C. J., Dennison, K. L., Klenchin, V. A., Rayment, I., and Escalante-Semerena, J. C. (2008) Construction and use of new cloning vectors for the rapid isolation of recombinant proteins from *Escherichia coli*. *Plasmid 59*, 231–237.
23. St Maurice, M., Mera, P. E., Taranto, M. P., Sesma, F., Escalante-Semerena, J. C., and Rayment, I. (2007) Structural characterization of the active site of the PduO-type ATP:Co(I)rrinoid adenosyltransferase from *Lactobacillus reuteri*. *J. Biol. Chem. 282*, 2596–2605.

24. Blommel, P. G., and Fox, B. G. (2007) A combined approach to improving large-scale production of tobacco etch virus protease. *Protein Expression Purif. 55*, 53–68.
25. Hall, D. A., Jordan-Starck, T. C., Loo, R. O., Ludwig, M. L., and Matthews, R. G. (2000) Interaction of flavodoxin with cobalamin-dependent methionine synthase. *Biochemistry 39*, 10711–10719.
26. Fonseca, M. V., and Escalante-Semerena, J. C. (2001) An in vitro reducing system for the enzymic conversion of cobalamin to adenosylcobalamin. *J. Biol. Chem. 276*, 32101–32108.
27. Otwinowski, Z., and Minor, W. (1997) Processing of X-ray diffraction data collected in oscillation mode. *Methods Enzymol. 276*, 307–326.
28. Vagin, A., and Teplyakov, A. (1997) *J. Appl. Crystallogr. 30*, 1022–1025.
29. Murshudov, G. N., Vagin, A. A., and Dodson, E. J. (1997) Refinement of macromolecular structures by the Maximum-Likelihood Method. *Acta Crystallogr. D53*, 240–255.
30. Emsley, P., and Cowtan, K. (2004) Coot: Model-building tools for molecular graphics. *Acta Crystallogr. D60*, 2126–2132.
31. Escalante-Semerena, J. C., Suh, S. J., and Roth, J. R. (1990) *cobA* function is required for both de novo cobalamin biosynthesis and assimilation of exogenous corrinoids in *Salmonella typhimurium*. *J. Bacteriol. 172*, 273–280.
32. Suh, S., and Escalante-Semerena, J. C. (1995) Purification and initial characterization of the ATP:corrinoid adenosyltransferase encoded by the *cobA* gene of *Salmonella typhimurium*. *J. Bacteriol. 177*, 921–925.
33. Berkowitz, D., Hushon, J. M., Whitfield, H. J., Jr., Roth, J., and Ames, B. N. (1968) Procedure for identifying nonsense mutations. *J. Bacteriol. 96*, 215–220.
34. Schubert, H. L., and Hill, C. P. (2006) Structure of ATP-bound human ATP:cobalamin adenosyltransferase. *Biochemistry 45*, 15188–15196.
35. Fan, C., and Bobik, T. A. (2008) Functional characterization and mutation analysis of human ATP:Cob(I)alamin adenosyltransferase. *Biochemistry 47*, 2806–2813.
36. Marsh, E. N., and Holloway, D. E. (1992) Cloning and sequencing of glutamate mutase component S from *Clostridium tetanomorphum*. Homologies with other cobalamin-dependent enzymes. *FEBS Lett. 310*, 167–170.
37. Reitzer, R., Gruber, K., Jogl, G., Wagner, U. G., Bothe, H., Buckel, W., and Kratky, C. (1999) Glutamate mutase from *Clostridium cochlearium*: The structure of a coenzyme B12-dependent enzyme provides new mechanistic insights. *Struct. Folding Des. 7*, 891–902.
38. Cook, F. C., and Cleland, W. W. (2007) *Enzyme Kinetics and Mechanism*, Taylor & Francis Group, LLC, New York.
39. Liu, D., Williamson, D. A., Kennedy, M. L., Williams, T. D., Morton, M. M., and Benson, D. R. (1999) Aromatic side chain-porphyrin interactions in designed hemoproteins. *J. Am. Chem. Soc. 121*, 11798–11812.
40. Padovani, D., Labunska, T., Palfey, B. A., Ballou, D. P., and Banerjee, R. (2008) Adenosyltransferase tailors and delivers coenzyme B_{12}. *Nat. Chem. Biol. 4*, 194–196.
41. Lerner-Ellis, J. P., Gradinger, A. B., Watkins, D., Tirone, J. C., Villeneuve, A., Dobson, C. M., Montpetit, A., Lepage, P., Gravel, R. A., and Rosenblatt, D. S. (2006) Mutation and biochemical analysis of patients belonging to the cblB complementation class of vitamin B12-dependent methylmalonic aciduria. *Mol. Genet. Metab. 87*, 219–225.

BI9000134